Journal of Hepatocellular Carcinoma

Dovepress
Taylor & Francis Group

Open Access Full Text Article

ORIGINAL RESEARCH

A Reproducible MRI-Based Quantitative Feature for Differentiating Dysplastic Nodules from Hepatocellular Carcinoma: A Multicenter Retrospective Study

Cheng Zhang[1,*], Shuyi Xie[1,*], Chuangxin Wang[1,*], Tuo Ren[2], Xi Zhong[3], Yixin Zhang[4], Shuo Li[1], Weijie Wu[5], Ying Sun[1], Chuanmiao Xie[1]

[1]Department of Radiology, Sun Yat-Sen University Cancer Center, Guangzhou, Guangdong, People's Republic of China; [2]Department of Radiology, The First Affiliated Hospital of Sun Yat-Sen University, Guangzhou, Guangdong, People's Republic of China; [3]Department of Radiology, Affiliated Cancer Hospital and Institute of Guangzhou Medical University, Guangzhou, Guangdong, People's Republic of China; [4]Shenzhen Key Laboratory for Systems Medicine in Inflammatory Diseases, Sun Yat-Sen University, Shenzhen, Guangdong, People's Republic of China; [5]Department of Radiology, The Sixth People's Hospital of Huizhou, Huizhou, Guangdong, People's Republic of China

*These authors contributed equally to this work

Correspondence: Chuanmiao Xie; Ying Sun, Email xchuanm@sysucc.org.cn; sunying@sysucc.org.cn

Purpose: High percentage of well-differentiated hepatocellular carcinoma (HCC) was radiologically misdiagnosed as dysplastic nodule (DN), which may lead to delay in treatment. This study aims to develop a reproducible feature for DN/HCC differentiation.

Patients and Methods: This study included patients which underwent curative hepatectomy or biopsy from four hospitals in China. The study population was divided into internal training cohort, internal test cohort, external validation cohort. Energy value was extracted from arterial and hepatobiliary phase lesion to represent intensity. Hepatobiliary-Arterial Intensity Ratio (HAIR) was calculated to demonstrate the intensity change from cirrhotic nodule to HCC. GPC3 (Glypican-3) was analyzed to validate HAIR's relation with nodule differentiation. Supporting Vector Machine (SVM) was built as a comparative model. Area Under the Curve (AUC) was used to evaluate and compare the predictive efficacy of HAIR.

Results: A total of 116 patients with 120 lesions (52 dysplastic nodules and 68 hepatocellular carcinomas) were included. The AUC of HAIR and SVM for differentiating DN and HCC in internal test cohort were 0.824 (95% CI, 0.662–0.986, $p<0.01$) and 0.733 (95% CI, 0.593–0.872, $p<0.01$), respectively. The cut-off value of the HAIR logistic regression based on training cohort was 0.46, which was subsequently validated in the external validation group. The AUC of HAIR in external validation cohort was 0.667. The correlation between HAIR and GPC3 showed statistical significance ($p<0.01$).

Conclusion: HAIR based on arterial and hepatobiliary phase provides a quantitative, reproducible and interpretable tool for DN/HCC differentiation.

Keywords: dysplastic nodule, hepatocellular carcinoma, magnetic resonance imaging, quantitative imaging feature, reproducibility

Introduction

Hepatocellular carcinoma (HCC) is one of the most common malignancies worldwide.[1] Cirrhosis is a high-risk factor for HCC occurrence. Pathologically, the hepatocarcinogenesis of HCC in cirrhosis patients is a multistep process, including cirrhotic regenerative nodule, low-grade dysplastic nodule (DN), high-grade dysplastic nodule, well-differentiated hepatocellular carcinoma, and advanced hepatocellular carcinoma.[2]

It usually takes several years for RN to progress into DN, which is a borderline tumor. However, well-differentiated HCC progresses rapidly to advanced HCC at a median time of 12 months.[3–6] Thus, precise differential diagnosis of DN and well-differentiated HCC is crucial for early clinical treatment decisions.

https://doi.org/10.2147/JHC.S609066
Received: 13 March 2026
Accepted: 7 May 2026
Published: 12 May 2026

Although liver tissue biopsy is the gold standard for distinguishing DN and well-differentiated HCC, it is an invasive examination.[7,8] Therefore, radiological examinations are widely adopted for hepatic nodule diagnosis. Yet there were still about 23% of well-differentiated HCC that were misdiagnosed as DN radiologically.[9,10] According to Guidelines for the Diagnosis and Treatment of Primary Liver Cancer, hepatic nodules ≤2 cm without or with one malignant radiological signatures are managed according to different doctors' treatment decisions (liver biopsy or follow-up).[11] Misdiagnosis of well-differentiated HCC may lead to delay in treatment, consequently influencing the prognosis of patients.

Gadoxetic acid-enhanced Magnetic Resonance imaging (Gd-EOB-MRI), with both early vascular phases and hepatobiliary phase using hepatocyte-specific contrast agent, is an effective modality for liver nodule characterization.[12,13] However, semantic imaging features derived from EOB-MRI still demonstrate relatively high misdiagnosis rate for DN and well-differentiated HCC differentiation, with inevitable subjectiveness.[6,14,15]

In recent decade, radiomics is a technique which can quantify the heterogeneity of tumors, with objectiveness for clinical research and practice. The quantified radiomic features are subsequently utilized for machine learning model construction.[16] However, many radiomics models suffer from poor reproducibility and interpretability, restricting clinical translation.[17–19] Selected features and model results may differ in different training and test cohort. And the operating principle of the constituent radiomic features in these predictive models cannot be related to subtle changes in micro-environment and tumor cells.

Therefore, this study aimed to develop a reproducible and interpretable MRI-based quantitative feature for differentiating dysplastic nodules from well-differentiated hepatocellular carcinoma. In addition, this study further validated the feature's relation with tumor cell differentiation, meanwhile comparing the feature's diagnostic efficacy with conventional radiomic machine learning models derived from arterial phase and hepatobiliary phase, respectively.

Materials and Methods

Study Population

Institutional Review Board of Sun Yat-sen University Cancer Center's approval was obtained. The approval number is B-2025-610-01, approval date was 2025–09-23. Written informed consent was not required for this study because this was a retrospective and observational study. The study was conducted in accordance with the Declaration of Helsinki. Patents' data that support the findings of this study are available from the corresponding author upon reasonable request. A total of 120 consecutive lesions were included from 4 independent hospitals between 2022 and 2024.

The inclusion criteria for all the centers were as follows:

1. Pathologically confirmed DN or well-differentiated HCC
2. Tumor maximum diameter ≤30mm (Atypical imaging features are seen in cirrhotic nodules ≤30mm, which may lead to misdiagnosis[20])
3. Available arterial phase and hepatobiliary phase MR images before treatment

The exclusion criteria for all the centers were as follows:

1. DN and HCC occurring in one liver nodule
2. Tumor maximum diameter >30mm
3. Incomplete clinical and follow-up data
4. MR images with apparent artifacts

Preoperative laboratory characteristics include white blood cell, albumin, total bilirubin, alpha-fetoprotein (AFP), hepatitis B virus DNA (HBV). Imaging features include tumor maximum length. Pathological data include cirrhosis. Imaging features include tumor maximum diameter. The flowchart of the overall research process is shown in Figure 1.

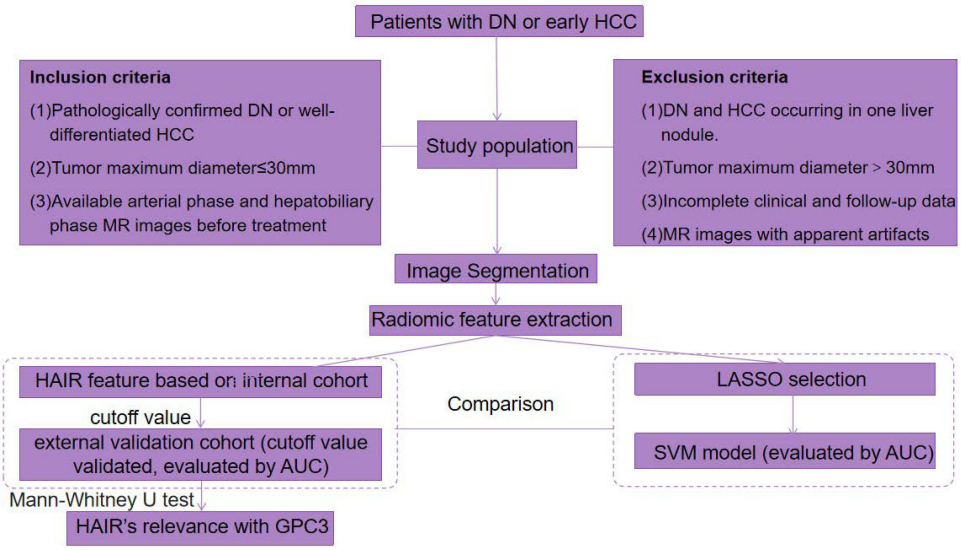

Figure 1 Flow chart of the overall study.

MRI Protocol

All MR images were acquired using 3.0-T MRI scanners. The detailed information of each scan sequence was shown in Table 1. All patients needed a food-fast of more than 6 hours and a water-fast of more than 4 hours before scanning. A dose of intracellular Gd contrast agent of 25 μmol per kg of body weight was manually administered bolus rapidly. It was immediately followed by 30 mL saline at a rate of 1 mL/s. The total injection process was under managed of the compressed sensing system. The arterial phases (AP), hepatobiliary phase (HBP) images were obtained during suspended respiration at 30–35 sec, and 20 min, respectively, under bolus track technique. We retrieved the arterial phase, hepatobiliary phase images from picture archiving and communication system (PACS) in Digital Imaging and Communications in Medicine (DICOM) format.

Reproducible Quantitative Feature Calculation

The discovery of the reproducible feature was based on the intensity change in arterial phase and hepatobiliary phase during the process from DN to well-differentiated HCC. During this process, the liver nodule may demonstrate increasingly high intensity in arterial phase, while it may demonstrate increasingly low intensity in hepatobiliary phase. According to the intensity change tendency of the two phases, we drew an assumption that there should be a cut-off value of the two phases' intensity ratio that can effectively distinguish DN and well-differentiated HCC.

Table 1 Details of MRI Protocol

		TR	TE	FOV	Matrix
SYSUCC	AP	4.21	1.93	360×247	352×194
	HBP	4.21	1.93	360×247	352×194
SYSUFAH	AP	3.6	1.32	400×340	320×205
	HBP	3.7	1.32	400×340	320×227
GZ8PH	AP	4.21	1.93	360×247.68	352×281.6
	HBP	4.21	1.93	360×247.68	352×281.6
GZCH	AP	4.5	2.3	440×352	320×224
	HBP	5.6	2.1	360×288	320×224

Abbreviations: SYSUCC, Sun Yat-sen University Cancer Prevention Center; SYSUFAH, Sun Yat-sen University First Affiliated Hospital; GZ8H, Guangzhou Eighth People's Hospital; GZCH, Guangzhou Cancer Hospital; AP, arterial phase; HBP, hepatobiliary phase.

https://doi.org/10.2147/JHC.S609066

Therefore, we utilized the original energy feature of first-order radiomic features to quantify the intensity of liver nodules in MR.[21] It is a measure of the magnitude of voxel values in an image. A larger values implies a greater sum of the squares of these values. The energy value ratio of the two phases may to some extent reduce the bias caused by tumor size in different lesions.

HAIR = Energy (HBP)/Energy (AP).

The Volume of Interest (VOI) was delineated by two radiologists (both with 6 years of abdominal radiology experience). The Intra- and Inter-observer coefficient was calculated to ensure the reproducibility of the VOI. The energy value of nodules was extracted from the VOI through Pyradiomics. Consequently, the reproducible feature Hepatobiliary-Arterial Intensity Ratio (HAIR) was calculated.

Radiomic Features Extraction and Model Construction of Comparative Radiomic Machine Learning Model

For comparative radiomic machine learning model, the radiomic features were extracted from all VOI segmentation through Pyradiomics, including first order, shape, texture features (gray level co-occurrence matrix; GLCM, gray level run length matrix, GLRLM; gray-level size zone matrix, GLSZM; gray-level dependence matrix, GLDM; neighboring gray tone dependence matrix, NGTDM; local binary pattern, LBP). The extracted features were selected using Least Absolute Shrinkage and Selection Operator (LASSO). The selected features were utilized for Supporting Vector Machine (SVM) model construction.

SVM is a supervised learning algorithm that classifies data by finding the best hyperplane to separate it.[22] It can handle both linear and nonlinear data and solve nonlinear problems by mapping the data to a high-dimensional space. Different types of data can be flexibly processed through kernel functions. Therefore, it performs well for small sample data. The kernel type used in this study is linear.

GPC3 Status for HAIR Interpretability

Glypican 3 (GPC3) is a generally acknowledged immunochemical staining biomarker for HCC. Its expression level represents the differentiation degree of tumor cells in liver nodules.[23] Hence, this study performed GPC3 immunochemical staining in all samples included. Subsequently, the correlation between HAIR feature and GPC3 status was statistically tested in the internal cohort to validate the interpretability of HAIR feature in microenvironmental and cellular aspects.

The GPC3 immunochemical staining status of liver nodules was categorized into three subtypes:[24]

a. Positivity: Positive expression of GPC3 was defined as cell membrane staining TC $\geq$ 10%. This means that in an immunohistochemical test, if the intensity of GPC3 staining on the cell membrane is 10% or more, the sample can be considered positive for GPC3.
b. Low Positivity: Low positive expression of GPC3 was defined as cell membrane staining 0% < TC < 10%. This means that in an immunohistochemical (IHC) test, if the intensity of GPC3 staining on the cell membrane is identified but less than 10%, the sample can be considered low positive for GPC3.
c. Negativity: Negative expression of GPC3 was defined as cell membrane staining TC = 0%. This means that in an immunohistochemical (IHC) test, if the intensity of GPC3 staining on the cell membrane is not identified, the sample can be considered negative for GPC3.

The demonstration of GPC3 status is shown in Figure 2.

Statistic Analysis

All statistical tests were performed using ShuKun Research Platform. Selection of radiomic features was done using the least absolute shrinkage and selection operator (LASSO). Logistic Regression was used to evaluate the diagnostic efficacy of HAIR feature and cut-off value was calculated from the logistic regression of training cohort for external validation. Supporting

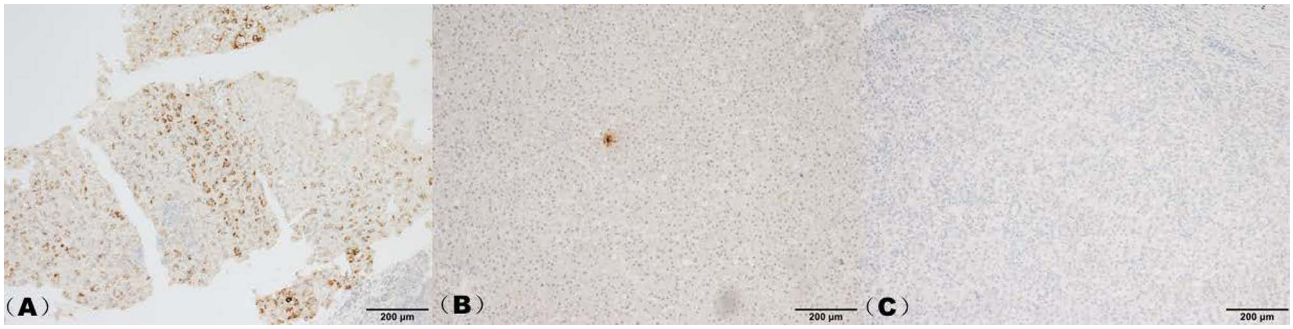

Figure 2 Demonstration of different immunochemical staining GPC3 status. (**A**) Positivity: Positive expression of GPC3 was defined as cell membrane staining TC ≥ 10%. (**B**) Low Positivity: Low positive expression of GPC3 was defined as cell membrane staining 0% < TC <10%. (**C**) Negativity: Negative expression of GPC3 was defined as cell membrane staining TC = 0%.

Vector Machine (SVM) was used to construct radiomic model for comparison due to its small sample size. Ten-fold cross validation was performed for HAIR and SVM model. Mann–Whitney *U*-test was performed to demonstrate the statistical relation between HAIR and GPC-3 status. Receiver operating characteristic curve (ROC), area under the ROC curve (AUC), sensitivity, specificity were calculated for the training, internal and external validation cohort of the HAIR signature and SVM model for further comparison. Calibration curves were plotted to compare the models' discriminating efficacy and the actual DN/HCC distribution. All statistical tests were two-sided, and $p<0.05$ was considered statistically significant.

Results

Baseline Characteristics of Study Cohorts

Due to limited sample size, eventually lesions with diameter>30mm were also included. A total of 116 consecutive patients were included. These patients have 120 lesions in total (68 HCCs and 52 DNs), from 4 independent hospitals between 2022 and 2024: Sun-Yat sen University Cancer Center (Internal cohort, n=87, 1 patient has 3 DNs, 2 patients have 2 DNs respectively), Guangzhou Eighth People's Hospital (n=6), Guangzhou Cancer Hospital (n=14), Sun Yat-sen First Affiliated Hospital (n=13). The baseline characteristics of the internal and external cohort are shown in Table 2 and Table 3. The internal cohort was randomly divided into internal training cohort and internal test cohort according to the ratio of 7:3.

Table 2 Baseline Characteristics of the Study Population (Internal Cohort)

Patients	DN Patients (n=37)	HCC Patients (n=46)	P value
Age	56.1 (22–69)	59.3 (18–79)	0.1747
Gender			0.8636
Male	33 (89.2)	41 (89.1)	
Female	4 (10.8)	5 (10.9)	
Liver disease			0.9668
HBV	34 (91.9)	36 (78.3)	
HCV	1 (2.7)	0 (0)	
None	6 (16.2)	7 (15.2)	
WBC	5.9 (3.46–9.57)	6.5 (2.61–11.85)	0.1415
ALB	43.7 (35.8–52.6)	44.7 (35.7–52.4)	0.25
TBIL	14.3 (5.1–30.6)	14.3 (5.4–37.1)	0.9718
AFP	80.2 (2.3–860)	2896.5 (1.12–55,558)	0.1223
Diameter (mm)	31 (9–65)	39.7 (11–111)	0.0598
Splenomegaly/Cirrhosis			0.8761
Splenomegaly (%)	12 (32.4)	6 (13.0)	
Cirrhosis (%)	27 (73.0)	21 (45.7)	
None	9 (24.3)	25 (54.3)	

Abbreviations: DN, dysplastic nodule; HCC, hepatocellular carcinoma; HBV, hepatitis B virus; HCV, hepatitis C virus; WBC, white blood cell; ALB, Albumin; TBIL, Total Bilirubin; AFP, α-fetoprotein.

https://doi.org/10.2147/JHC.S609066

Table 3 Baseline Characteristics of the Study Population (External Cohort)

Patients	DN Patients (n=11)	HCC Patients (n=22)	P value
Age	59.9 (50–75)	61.8 (49–101)	0.708
Gender			0.555
Male	9 (81.8)	18 (81.8)	
Female	2 (18.2)	4 (18.2)	
Liver disease			0.687
HBV	11 (100.0)	21 (95.5)	
HCV	1 (9.1)	0	
None	0	1 (4.5)	
WBC	5.8 (2.97–7.86)	5.4 (1.91–10.6)	0.7635
ALB	40 (35.1–46.7)	40.1 (24.8–50.8)	0.9618
TBIL	17.7 (4.5–43.8)	15.1 (6.9–30.2)	0.415
AFP	75.7 (1.24–726.83)	87.9 (2.35–866)	0.8704
Diameter (mm)	21 (9–78)	26 (10–86)	0.5531
Splenomegaly/Cirrhosis			0.2729
Splenomegaly (%)	5 (45.5)	7 (31.8)	
Cirrhosis (%)	8 (72.7)	13 (59.1)	
None	3 (27.3)	6 (27.3)	

Abbreviations: DN, dysplastic nodule; HCC, hepatocellular carcinoma; HBV, hepatitis B virus; HCV, hepatitis C virus; WBC, white blood cell; ALB, Albumin; TBIL, Total Bilirubin; AFP, α-fetoprotein.

Construction of HAIR Feature and Radiomic SVM Model

According to original energy value extracted from the VOI of lesions, the HAIR feature of the training cohort was calculated as the energy value ratio of hepatobiliary phase and arterial phase. The cut-off value of the HAIR logistic regression model was 0.46.

One hundred and sixteen radiomic features were extracted from the VOI of the lesions in training cohort. Subsequently, LASSO selected 7 radiomic features with non-zero coefficients and Intra- and Inter-observer coefficient greater than 0.8, the selected features were considered relevant with DN/HCC classification. Eventually, the selected features were used for SVM model construction.

Diagnostic Efficacy of HAIR and Radiomic Model in Training Cohort and Internal Test Cohort

The ROC curves of HAIR logistic regression and radiomic SVM model in training and internal test cohort are shown in Figure 3. The calibration curves of HAIR logistic regression and radiomic SVM models are shown in Figure 4. The AUC of HAIR and SVM models for differentiating DN and HCC in training cohort were 0.828 (95% CI, 0.723–0.933) and 0.764 (95% CI, 0.681–0.848), respectively. The AUC of HAIR and SVM models for differentiating DN and HCC in internal test cohort were 0.824 (95% CI, 0.662–0.986) and 0.733 (95% CI, 0.593–0.872), respectively. The sensitivity, specificity, accuracy of HAIR features in the internal test cohort were 0.643, 0.846, 0.741, respectively. The sensitivity, specificity, accuracy of radiomic SVM model in internal test cohort were 0.393, 0.840, 0.604, respectively.

Diagnostic Efficacy of HAIR Feature in External Validation Cohort

The ROC curves of HAIR logistic regression and radiomic SVM model in training and internal test cohort are shown in Figure 5. The cut-off value derived from HAIR features in the training cohort was subsequently validated in the external validation group. The AUC of HAIR in external validation cohort was 0.667 (95% CI, 0.426–0.908), and the sensitivity, specificity, accuracy of HAIR feature in external validation cohort were 0.571, 0.727, 0.625, respectively. As a single interpretative imaging feature.

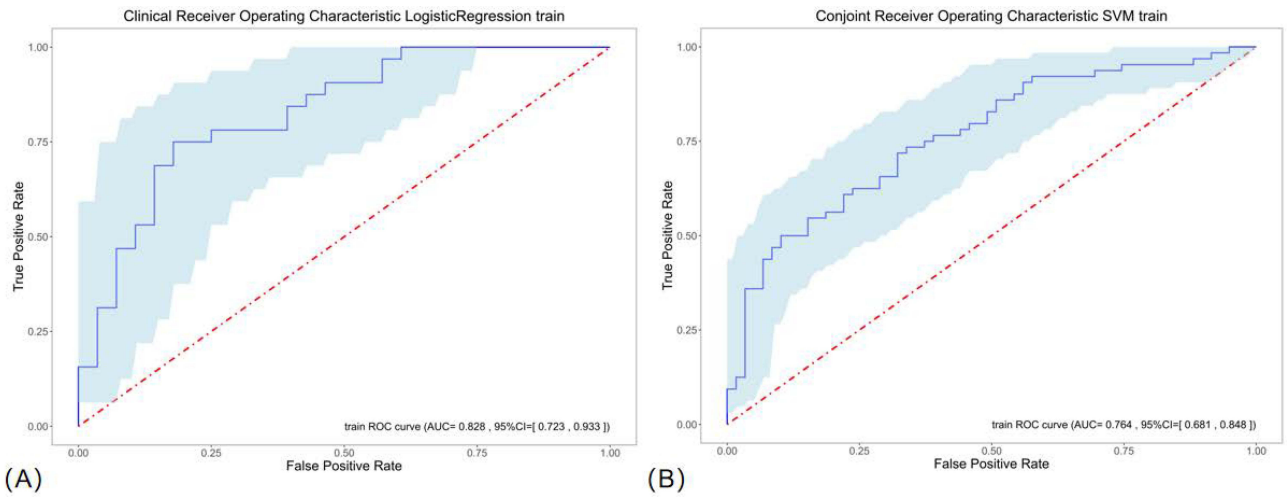

Figure 3 (**A**) Receiver Operating Characteristics curve of HAIR feature in training cohort. (**B**) Receiver Operating Characteristics curve of SVM model in training cohort.

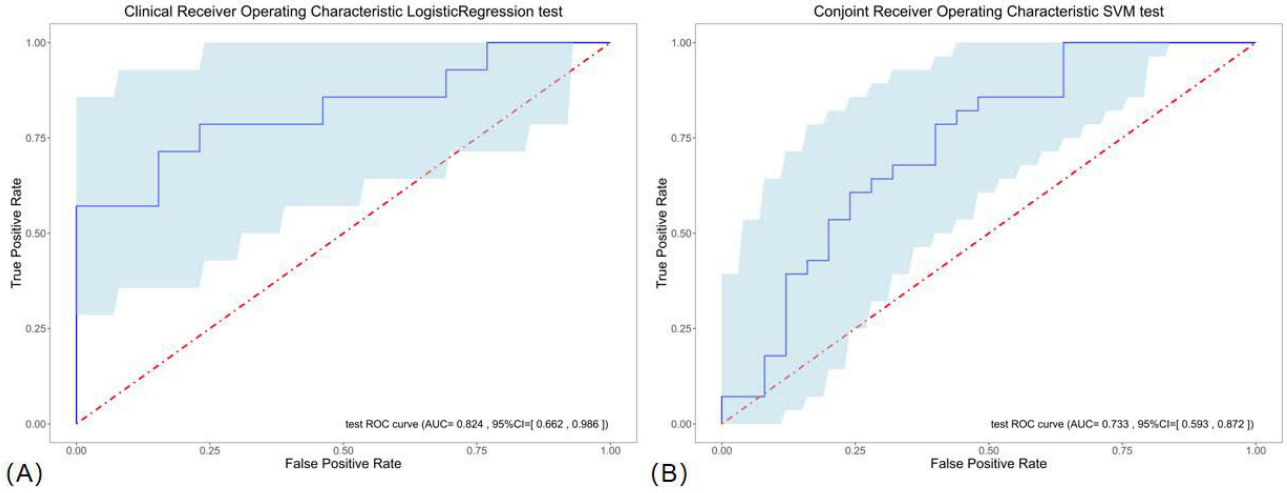

Figure 4 (**A**) Receiver Operating Characteristics curve of HAIR feature in internal test cohort. (**B**) Receiver Operating Characteristics curve of SVM model in internal test cohort.

Correlation Between HAIR and GPC3 Status

Kruskal–Wallis test was performed for evaluating correlation between HAIR and immuno-histochemical staining GPC3 status. The distribution of different GPC3 statuses in the training cohort and statistical analysis result are demonstrated in Table 4 and Figure 6. The correlation between HAIR feature and GPC3 status showed statistical significance ($p<0.001$).

Discussion

In this multi-center study, we built a special quantitative image feature HAIR for DN and HCC differentiation. The feature achieved well performance for DN/HCC differentiation. And we further compared HAIR with conventional radiomic machine learning model based on arterial phase and hepatobiliary phase. HAIR achieved better performance in either training cohort, internal test cohort and external validation cohort.

Since HAIR feature is directly calculated from the extracted energy value from arterial phase and hepatobiliary phase images, it demonstrates better reproducibility than conventional radiomic model. Meanwhile, we tested the correlation between HAIR and GPC3 status, the result validated that HAIR is related to tumor differentiation in micro-environmental aspect. Therefore, our study may provide a simple ancillary tool for DN/HCC differentiation, with greater reproducibility and intepretability.

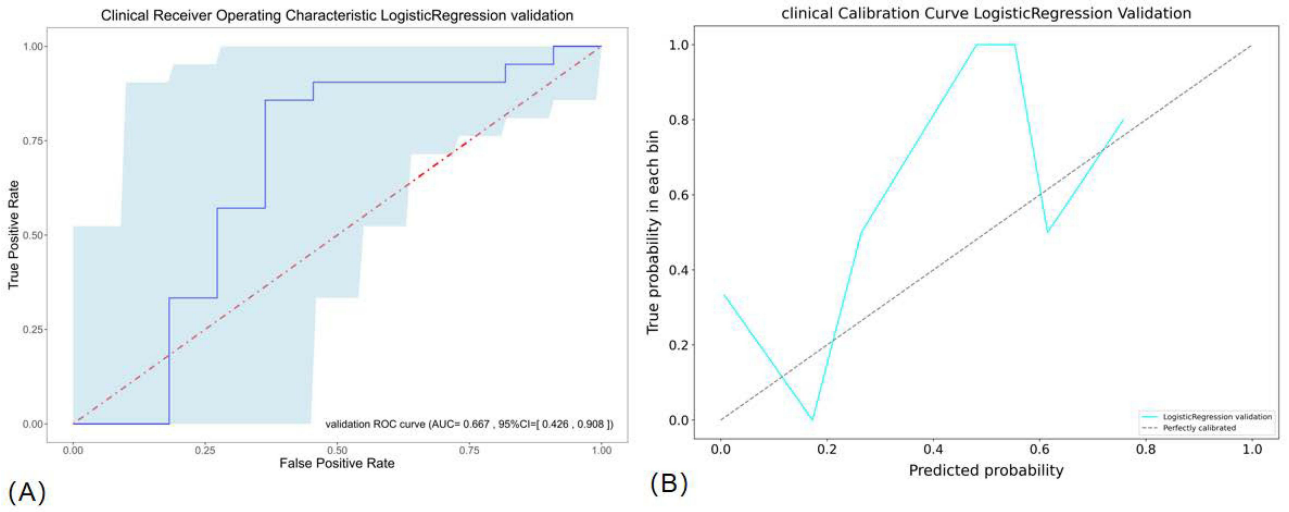

Figure 5 (**A**) Receiver Operating Characteristics curve of HAIR feature in external validation cohort. (**B**) Calibration curve of HAIR feature in external validation cohort.

The differential diagnosis of DN and well-differentiated HCC was mainly done by radiologists according to semantic imaging features, while the misdiagnosis rate approached 23% in certain procedure due to lesions' heterogeneity. The treatment method for small suspicious liver nodules was decided by attending physicians (close follow-up or biopsy). Thus misdiagnosis may lead to delayed treatment for early HCC, consequently resulting in poorer prognosis. A few radiological studies attempted to differentiate DN and HCC through quantitative modalities. Chen used T1 mapping on MR for DN/HCC differentiation. In the study, the AUCs of T1hp, ΔT1, CVT1-hp, and ΔT1% in identifying HCC from DN were 0.955, 0.910, 0.932, 0.818, respectively.[25] However, despite the single center essence of this study, T1 mapping is performed on original MR images without processing, which indicates that the study cohort should be prospectively collected. Due to the rarity of pathologically diagnosed DN in clinical practice, the application of this technology on DN/HCC differentiation may lack clinical translational value. For retrospective study, Zhong used texture analysis based on hepatobiliary phase (HBP) and diffusion-weighted images (DWI) for DN/HCC differentiation. The AUC of their combined model (HBP+DWI) reached an AUC of 0.96.[26] Yet the texture analysis model still retains the reproducibility and interpretability problems occurring in most of the radiomic studies in recent years.[27] The performance of certain constructed models may not perform equivalently well in external validation cohort. In fact, selected features for specific study purpose may even vary in different centers. Furthermore, the correlation between the selected texture features and tumor differentiation could not be properly interpreted. Based on a multi-center study cohort, our study discovered a reproducible quantitative MR feature with good diagnostic performance for DN/HCC differentiation, after which we identified the internal correlation between HAIR and tumor differentiation through immunohistochemical staining biomarker GPC3, confirming the biological relevance of HAIR feature. This feature is not only a significant method for reducing misdiagnosis, but also an important tool for early HCC detection and cirrhotic nodule surveillance. Nodules with high risk after HAIR evaluation may subsequently undergo biopsy or curative surgery or ablation in clinical procedure, which may influence patients' prognosis.

Table 4 Distribution of Different GPC3 Status in the Internal Cohort

GPC3 (Median)	**Ratio**
1.0 (n=50)	0.716
2.0 (n=10)	1.532
3.0 (n=27)	4.605
The Kruskal–Wallis test H value	15.417
p	<0.001

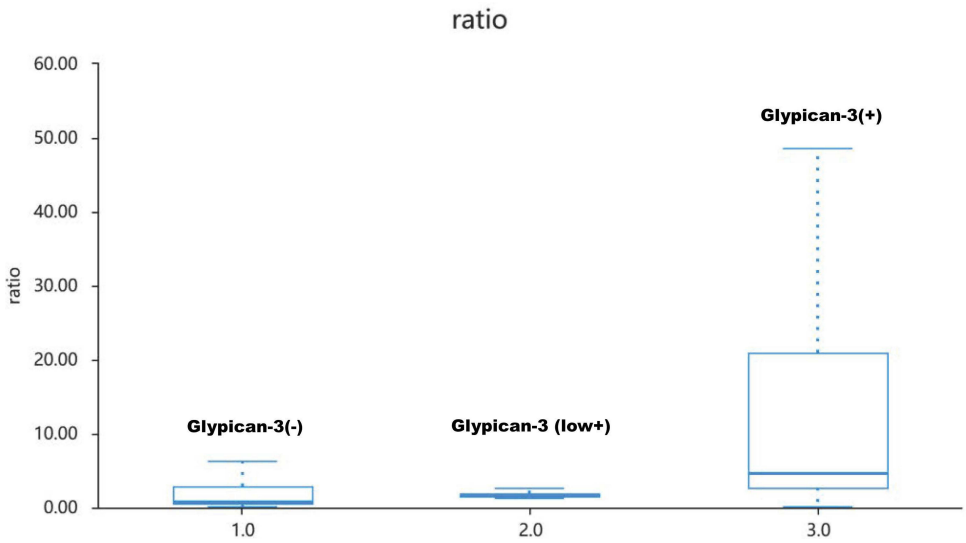

Figure 6 Box-plot showing the distribution of different GPC3 status in internal cohort.

The construction of HAIR also provided a methodological reference for retrospective MR studies. Previous MR studies could not objectively quantifies signal intensity of VOI owing to the bias caused by various MR scanners and parameters. Our study used energy value as a way for quantifying VOI intensity. According to intensity changes of cirrhotic liver nodules in hepatobiliary phase and arterial phase, we utilized energy value ratio of the two phases to simultaneously represent tumor progression and minimize the bias caused by tumor volume. This shows that the proper calculation method of energy value derived from clinical experience may become a novel way for lesion MR intensity quantification. With similar methods, a radiological follow-up system for cirrhotic nodules will hopefully be built in future studies.

This study also has several limitations. First, pathologically diagnosed DNs are rare in clinical practice. Though the cohort included in this study was relatively sufficient compared to other radiology studies involving DN, the sample size was still not adequate for machine learning models. In future studies with larger sample size and more centers, the diagnostic efficacy of HAIR may be comprehensively demonstrated. Second, this study only explored the biological significance of HAIR through its relevance with GPC3 status. If the relation between HAIR and OATP receptor expression in tumor can be further validated, HAIR feature will have substantial biological significance and interpretability. Third, this is a retrospective study. The lesions were manually segmented. These may lead to inevitable bias in the result. Lastly, this study did not explored the inter-phases calculation of other radiomic features for DN/HCC differentiation. With the basis of HAIR feature calculation, the inter-phases calculation of other radiomic features may be beneficial for the construction of cirrhosis liver nodule follow-up system.

Conclusion

In this multi-center study, we discovered a quantitative imaging feature HAIR for the differentiation of DN and well-differentiated HCC with good reproducibility. The HAIR feature achieved good performance and its biological significance was validated. This interpretable and reproducible imaging feature may serve as a useful tool for the surveillance and early diagnosis of cirrhotic liver nodules.

Patients Data Confidentiality Statement

All patient data was handled confidentially.

Abbreviations

AUC, area under the ROC curve; AFP, alpha-fetoprotein; DICOM, Digital Imaging and Communications in Medicine; DN, dysplastic nodule; HCC, hepatocellular carcinoma; FOV, field of view; Gd-EOB-MRI, Gadoxetic acid-enhanced Magnetic

Resonance imaging; GLCM, gray level co-occurrence matrix; GLRLM, gray level run length matrix; GLSZM, gray-level size zone matrix; GLDM, gray level dependence matrix; GPC3, Glypican-3; HAIR, Hepatobiliary-Arterial Intensity Ratio; AP, arterial phase; HBP, hepatobiliary phase; HBV, hepatitis B virus; LASSO, Least Absolute Shrinkage and Selection Operator; LBP, local binary pattern; NGTDM, neighboring gray tone dependence matrix; PACS, picture archiving and communication system; ROC, Receiver operating characteristic curve; SVM, Supporting Vector Machine; VOI, Volume of Interest.

Disclosure

The authors of this manuscript declare no conflict of interests in this work.

References

1. Bray F, Ferlay J, Soerjomataram I, Siegel RL, Torre LA, Jemal A. Global cancer statistics 2018: GLOBOCAN estimates of incidence and mortality worldwide for 36 cancers in 185 countries. *CA Cancer J Clin*. 2018;68(6):394–424. doi:10.3322/caac.21492
2. Choi BI, Takayasu K, Han MC. Small hepatocellular carcinomas and associated nodular lesions of the liver: pathology, pathogenesis, and imaging findings. *AJR Am J Roentgenol*. 1993;160(6):1177–1187. doi:10.2214/ajr.160.6.8388618
3. Takayama T, Yamazaki S, Kosuge T, et al. Malignant transformation of adenomatous hyperplasia to hepatocellular carcinoma. *Lancet*. 1990;336 (8724):1150–1153. doi:10.1016/0140-6736(90)92768-D
4. Sakamoto M, Hirohashi S, Shimosato Y. Early stages of multistep hepatocarcinogenesis: adenomatous hyperplasia and early hepatocellular carcinoma. *Hum Pathol*. 1991;22(2):172–178. doi:10.1016/0046-8177(91)90039-R
5. Villanueva A. Hepatocellular carcinoma. *N Engl J Med*. 2019;380(15):1450–1462. doi:10.1056/NEJMra1713263
6. Di Tommaso L, Sangiovanni A, Borzio M, Park YN, Farinati F, Roncalli M. Advanced precancerous lesions in the liver. *Best Pract Res Clin Gastroenterol*. 2013;27(2):269–284. doi:10.1016/j.bpg.2013.03.015
7. Russo FP, Imondi A, Lynch EN, Farinati F. When and how should we perform a biopsy for HCC in patients with liver cirrhosis in 2018 A review. *Dig Liver Dis*. 2018;50(7):640–646. doi:10.1016/j.dld.2018.03.014
8. Pang EH, Harris AC, Chang SD. Approach to the solitary liver lesion: imaging and when to biopsy. *Can Assoc Radiol J*. 2016;67(2):130–148. doi:10.1016/j.carj.2015.07.005
9. van der Pol CB, McInnes MDF, Salameh JP, et al. CT/MRI and CEUS LI-RADS major features association with hepatocellular carcinoma: individual patient data meta-analysis. *Radiology*. 2022;302(2):326–335. doi:10.1148/radiol.2021211244
10. Yang JD, Heimbach JK. New advances in the diagnosis and management of hepatocellular carcinoma. *BMJ*. 2020;371:m3544. doi:10.1136/bmj.m3544
11. Zhou J, Sun H, Wang Z, et al. Guidelines for the diagnosis and treatment of primary liver cancer (2022 edition). *Liver Cancer*. 2023;12(5):405–444. doi:10.1159/000530495
12. Ahn SS, Kim MJ, Lim JS, Hong HS, Chung YE, Choi JY. Added value of gadoxetic acid-enhanced hepatobiliary phase MR imaging in the diagnosis of hepatocellular carcinoma. *Radiology*. 2010;255(2):459–466. doi:10.1148/radiol.10091388
13. Kawada N, Ohkawa K, Tanaka S, et al. Improved diagnosis of well-differentiated hepatocellular carcinoma with gadolinium ethoxybenzyl diethylene triamine pentaacetic acid-enhanced magnetic resonance imaging and Sonazoid contrast-enhanced ultrasonography. *Hepatol Res*. 2010;40(9):930–936. doi:10.1111/j.1872-034X.2010.00697.x
14. Kogita S, Imai Y, Okada M, et al. Gd-EOB-DTPA-enhanced magnetic resonance images of hepatocellular carcinoma: correlation with histological grading and portal blood flow. *Eur Radiol*. 2010;20(10):2405–2413. doi:10.1007/s00330-010-1812-9
15. Kitao A, Matsui O, Yoneda N, et al. The uptake transporter OATP8 expression decreases during multistep hepatocarcinogenesis: correlation with gadoxetic acid enhanced MR imaging. *Eur Radiol*. 2011;21(10):2056–2066. doi:10.1007/s00330-011-2165-8
16. Gillies RJ, Kinahan PE, Hricak H. Radiomics: images are more than pictures, they are data. *Radiology*. 2016;278(2):563–577. doi:10.1148/radiol.2015151169
17. Klontzas ME. Radiomics feature reproducibility: the elephant in the room. *Eur J Radiol*. 2024;175:111430. doi:10.1016/j.ejrad.2024.111430
18. Akinci D'Antonoli T, Cavallo AU, Vernuccio F, et al; Radiomics Auditing Group. Reproducibility of radiomics quality score: an intra- and inter-rater reliability study. *Eur Radiol*. 2024;34(4):2791–2804. doi:10.1007/s00330-023-10217-x
19. Papadimitroulas P, Brocki L, Christopher Chung N, et al. Artificial intelligence: deep learning in oncological radiomics and challenges of interpretability and data harmonization. *Phys Med*. 2021;83:108–121. doi:10.1016/j.ejmp.2021.03.009
20. Shin SK, Kim YS, Choi SJ, et al. Contrast-enhanced ultrasound for the differentiation of small atypical hepatocellular carcinomas from dysplastic nodules in cirrhosis. *Dig Liver Dis*. 2015;47(9):775–782. doi:10.1016/j.dld.2015.05.001
21. Zwanenburg A, Leger S, Vallières M, Löck S. Image biomarker standardisation initiative - feature definitions. 2016. In eprint arXiv:1612.07003 [cs.CV].
22. Hsieh WW. *Machine Learning Methods in the Environmental Sciences: Neural Networks and Kernels*. Cambridge university press; 2009:157–169. Chapter 7.
23. Devan AR, Nair B, Pradeep GK, et al. The role of glypican-3 in hepatocellular carcinoma: insights into diagnosis and therapeutic potential. *Eur J Med Res*. 2024;29(1):490. doi:10.1186/s40001-024-02073-2
24. Shafizadeh N, Ferrell LD, Kakar S. Utility and limitations of glypican-3 expression for the diagnosis of hepatocellular carcinoma at both ends of the differentiation spectrum. *Mod Pathol*. 2008;21(8):1011–1018. doi:10.1038/modpathol.2008.85
25. Chen D, Guo Y, Ran Q, et al. Gd-EOB-DTPA-enhanced magnetic resonance imaging combined with T1 mapping identifies dysplastic module and hepatocellular carcinoma: a retrospective study. *Curr Med Imag*. 2023;20. doi:10.2174/1573405620666230808153145
26. Zhong X, Tang H, Lu B, et al. Differentiation of small hepatocellular carcinoma from dysplastic nodules in cirrhotic liver: texture analysis based on MRI improved performance in comparison over gadoxetic acid-enhanced MR and diffusion-weighted imaging. *Front Oncol*. 2020;9:1382. doi:10.3389/fonc.2019.01382
27. Horvat N, Papanikolaou N, Koh DM. Radiomics beyond the hype: a critical evaluation toward oncologic clinical use. *Radiol Artif Intell*. 2024;6(4): e230437. doi:10.1148/ryai.230437